Spring 5-1-2014

The Development of Novel Anti-folates: An Ongoing Battle Against Resistance

Nhi Tran
University of Connecticut - Storrs, nhi.tran@uconn.edu

The Development of Novel Anti-folates: An Ongoing Battle Against Resistance

Honors Scholar Thesis
May 2014

Nhi N. Tran
PharmD Candidate 2014
University of Connecticut

Research Advisor: Amy Anderson, PhD
Department of Pharmaceutical Sciences
University of Connecticut School of Pharmacy

Table of Contents

Abstract

The development of drug compounds begins with the identification of a well-validated target. Conserved in bacterial, fungal, and mammalian species, the folate biosynthetic pathway performs critical processes to promote nucleic acid synthesis and maintain cellular function. Medicinal chemists have particularly targeted dihydrofolate reductase (DHFR), an essential enzyme in this metabolic process, for several years. In fact, anti-folates that act on this pathway have potential roles against infectious diseases. This project examines a para-substituted drug compound called UCP111E, which is directed against dangerous fungal species, like *Candida albicans* and *Candida glabrata*. Since crystal structures of *C. albicans* DHFR (CaDHFR) and *C. glabrata* DHFR (CgDHFR) with UCP111E have already been solved, the main objective is to now deduce the structure of human DHFR (huDHFR) complexed with the drug compound.

Sample preparation procedures in this project used Qiagen EasyXtal 15-well trays to plate various conditions for crystallization. The buffer (i.e., Tris), salt (i.e., lithium sulfate), precipitant (i.e., PEG 4000), and additive (i.e., ethanol) remained constant for each well in the trays. However, non-volatile additives (i.e., 1,8-diaminooctane, strontium chloride, and calcium chloride) varied, with the initial focus being on 1,8-diaminooctane.

Several steps to improve the conditions with 1,8-diaminooctane produced plate-like crystals, while strontium chloride formed hexagon-shaped crystals, and calcium chloride, crystal rods. Only those crystals formed from 1,8-diaminooctane and calcium chloride were large enough to diffract. However, diffraction patterns revealed the presence of salt, rather than protein, in the structures. Future projects hope to continue optimizing conditions with strontium chloride and calcium chloride to crystallize the huDHFR/UCP111E complex.

Introduction

Infectious disease was the primary cause of death worldwide in the early 1900s (1). However, Alexander Fleming's accidental discovery of penicillin in 1928 triggered an enormous surge of antibiotic development in the 1930s. The first half of the twentieth century witnessed the advent of many antibacterial agents. Over the next thirty years, 14 different classes of antibiotics including beta-lactams, sulfonamides, aminoglycosides, tetracyclines, macrolides, and lincosamides, became available. After 1968 though, drug discovery drastically diminished, with the introduction of only about five more antibiotic classes (2). Equipped with these drugs, many assumed victory and thus, an end to the battle against infectious microorganisms. Unfortunately, bacteria have continually found new ways to fight back by undergoing mutations to subtly modify target enzymes, thereby conferring resistance. Other mechanisms of resistance, particularly in Gram-negative organisms, include the loss of porins, overexpression of efflux pumps, and creation of bypass targets, all of which help bacteria evade their imminent demise (1). Keeping pace with resistance mechanisms by creating new drug compounds is the only way to fight the ongoing war against the microbial world.

Antimicrobial resistance remains one of the greatest threats to human health across the globe. Formidable drug-resistant strains, including methicillin-resistant *Staphylococcus aureus* (MRSA), vancomycin-resistant *enterococcus* (VRE), *Pseudomonas aeruginosa,* extended-spectrum beta lactamase (ESBL) Gram-negative organisms, and *Klebsiella pneumoniae* carbapenemases (KPC), have resulted in significant morbidity and mortality. Nearly two million Americans annually develop hospital-acquired infections (HAI), like sepsis and pneumonia, which result in 99,000 deaths and cost the U.S. health care system billions of dollars. Over-prescription and inappropriate use of antibiotics also contribute to this worldwide dilemma by

making the medications less effective. In addition to the unnecessary and excessive antimicrobial use, people may also receive the wrong drug at incorrect doses or schedules (3). The current development of new medications exceedingly lags behind bacteria's natural ability to evolve and confer resistance. Therefore, the search for new antibiotics ultimately becomes more pressing.

Similarly, the incidence of opportunistic fungal infections (i.e., invasive candidiasis) has significantly increased over the past few decades and ranks as the fourth most common cause of hospital-acquired bloodstream infections in the United States (4). Immunocompromised individuals particularly suffer from excessive morbidity and mortality after contracting candidemia. Other high-risk patient populations include the elderly, premature babies, solid-organ transplant recipients, bone marrow transplant patients, and those undergoing major surgical procedures. *Candida albicans* and *Candida glabrata* remain two of the worst contenders in fungal infections. In fact, the incidence of candidiasis from *C. glabrata* has increased since 1993 (5). This strain even demonstrates resistance to amphotericin B and many azole compounds, thereby limiting the usefulness of current antifungal compounds.

The approval of novel antifungals appears almost as stagnant as that of antibacterial drugs. Amphotericin B, one of the earliest antifungal agents from the early 1950s, has activity against most fungi, but its infusion-related and renal toxicities somewhat limit its use. Other antifungals include flucytosine and griseofulvin from the early 1960s, azole compounds (i.e., ketoconazole, fluconazole, itraconazole, etc.) from the 1970s-80s, and caspofungin from the early 2000s. With very few antifungal drug classes available, the discovery of new molecular targets remains imperative to expand the currently limited repertoire (6).

Dihydrofolate reductase (DHFR), an essential enzyme in the folate biosynthetic pathway, has been a well-validated target not only for antibacterial therapeutics, but also for anticancer

and antiprotozoal agents, for over 60 years (7). In the folate pathway, DHFR uses NADPH as an electron donor to reduce dihydrofolate to tetrahydrofolate, leading to the synthesis of essential purines and amino acids. Consequently, blocking DHFR with anti-proliferative drug compounds leads to a deficiency in tetrahydrofolate and reduces cellular growth. Examples of such compounds include methotrexate, an anticancer agent, pyrimethamine, an antimalarial drug, and trimethoprim (Table 1 below), an antibacterial. Trimethoprim inhibits Gram-positive and Gram-negative organisms (i.e., *S. aureus*, *S. pyrogenes*, *S. pneumoniae*, *E. faecalis*, *E. Coli*, *K. pneumonia*, and *H. influenza*) *in vitro*. Since both mammalian and bacterial cells contain DHFR, drug compounds need both potency and selectivity. Trimethoprim fortunately has an IC_{50} value approximately 3000 times higher for human versus bacterial DHFR, allowing for more focused activity in infectious diseases (7). For urinary tract infections, trimethoprim has also been used in combination with sulfamethoxazole to block dihydropteroate synthetase, another folate pathway enzyme. Unfortunately, resistant bypass enzymes and point mutations have created resistance.

Table 1: Comparing Trimethoprim and UCP111E

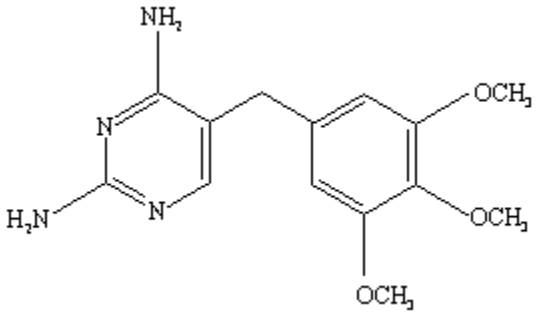	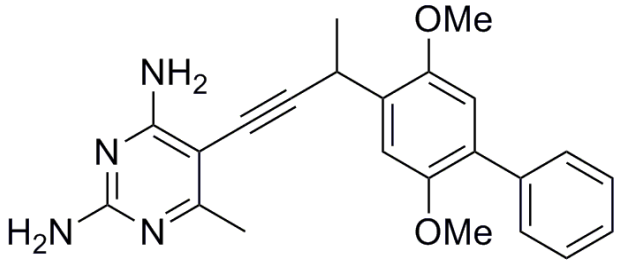
a. Trimethoprim	b. UCP111E

Bacterial resistance signals a need for additional structure-based drug design to synthesize novel anti-folates. Medicinal chemists have used trimethoprim (MW 290.32 g/mol) as

their base and began constructing propargyl-linked anti-folates to target DHFR. Trimethoprim's structure contains a di-substituted pyrimidine ring, methylene linker, and a phenyl ring with three methoxy groups. Further modifications began with the synthesis of compounds containing biphenyl groups attached to a propargyl linker. Chemists knew that the pyrimidine helped lock the compound in the DHFR active site, while the propargyl linker forced the hydrophobic biphenyl deeper into a hydrophobic pocket. They also experimented with the biphenyl to optimize hydrophobic interactions and binding. Specifically, para-substituted compounds potently inhibited CaDHFR and CgDHFR. In this project, UCP111E (MW 388.46 g/mol), one of the para-substituted compounds, is examined against huDHFR. This compound contains a pyrimidine ring system with two amino groups, a propargyl bridge, a benzene ring with two methoxy substitutions, and a para-substituted phenyl ring. As seen in Table 1 below, UCP111E has a higher IC_{50} value against huDHFR compared to CaDHFR and CgDHFR. Currently, the goal is to examine the binding properties of UCP111E with huDHFR to further increase selectivity and affinity for fungal DHFR. The two methoxy groups in the biphenyl system are of particular interest in UCP111E. Other compounds, like UCP111F, have very similar structures to UCP111E, with the only difference being a missing methoxy group from the aromatic ring. Many of the IC_{50} values for UCP111F were significantly higher than that of UCP111E, demonstrating less potent activity. The potency for huDHFR differed, but activity against CaDHFR and CgDHFR was similar.

Table 2: IC_{50} Values for DHFR

Drug Compound	IC_{50} for CaDHFR	IC_{50} for CgDHFR	IC_{50} for huDHFR
UCP111E	36 nM	8.2 nM	314 nM
UCP111F	55 nM	9.1 nM	1.42 uM

Materials and Methods

Protein Purification

BL21 DE3 E. coli competent cells were transformed with the huDHFR gene in the pET41a(+) plasmid. One-liter cultures of huDHFRpET41/BL21(DE3) were grown in LB media containing 50 µg/mL kanamycin at 37ºC. Once the cultures reached optical densities of 0.7 to 0.9 at 600 nm, a final concentration of 1mM isopropyl β-D-1-thiogalactopyranoside (IPTG) was added to each culture. Protein expression proceeded for 6 hours at 30ºC. The cells were then harvested by centrifugation and subsequently stored at -80°C.

One-liter cultures of huDHFRpET41/BL21(DE3) were dissolved in 1 x Bugbuster with DNase and 1mM PMSF. After incubation at room temperature, soluble lysate was collected via centrifugation. To remove contaminant proteins prior to chromatography, the soluble lysate was incubated in 60% saturation ammonium sulfate overnight at 4°C. The soluble crude protein sample was then added to a methotrexate column pre-equilibrated with Equilibration buffer (20 mM Tris, 15% (v/v) glycerol, 50 mM KCl, 2mM DTT, 0.1 mM EDTA, and 1mM PMSF). Contaminant proteins that did not bind methotrexate were washed from the column with Wash buffer (20 mM Tris, 15% (v/v) glycerol, 0.5 M KCl, 2mM DTT, 0.1 mM EDTA, and 1 mM PMSF). The column was subsequently re-equilibrated with Equilibration buffer. HuDHFR bound to methotrexate beads were eluted from the column with Elution buffer (20 mM Tris, 15% (v/v) glycerol, 50 mM KCl, 0.1 mM EDTA, 2mM DTT, and 1mM PMSF), and the column was washed with more Equilibration buffer. The fractions from the methotrexate column were evaluated using SDS-PAGE. Fractions containing huDHFR in excess of contaminants were pooled and concentrated for addition to an S200 column.

After further purification with the S200 column, protein was diluted with Desalting buffer to 8 mg/mL and flash frozen in liquid nitrogen.

Sample Preparation and Protein Crystallization. Crystals of huDHFR bound to UCP111E were grown using the hanging drop method on Qiagen EasyXtal 15-well trays. Various conditions were plated to determine the most optimal settings for crystal formation. The 500 µL of reservoir solution in each well contained the same basic components: Tris buffer, PEG 4000, lithium sulfate, and ethanol. The reservoir solution was prepared, allowed to mix, and stored at 4°C until the sample preparation.

For each plate, 4 µL each of 50mM NADPH and 50mM UCP111E stock (or 7.76 µL of 10 mg/mL UCP111E stock) were added to 200 µL aliquots of huDHFR (8 mg/mL) The solution was left to incubate on ice for 2 hours. Afterward, the contents of the tubes were filtered, centrifuged, and brought to the desired final protein concentration with Desalting buffer.

The prepared EasyXtal trays, along with Eppendorf tubes of the non-volatile additive and huDHFR, were placed on ice. Two microliters of reservoir solution, followed by 2 µL of huDHFR, were pipetted into each of the 3 cavities in the DropGuard Crystallization Support. Half a microliter of the corresponding concentrations of non-volatile additive was then added to each cavity, and the Crystallization Support was fastened to the well. After completion, the crystal tray was returned to 4°C for incubation.

Freezing Crystals. The wells that produced the most promising crystals were identified, and 1000 µL of cryoprotectant solution were made for each condition. Each cryoprotectant solution contained 500 µL of the respective reservoir solution, along with 150 µL ethylene glycol and 350 µL diH_2O. After the solutions were made, they were allowed to mix for a few hours before being stored at 4°C.

At 4 °C, crystals were harvested with Hampton Crystal Cap™ Copper Magnetic HT 0.2-0.3 mm CryoLoops, deposited into the corresponding cryoprotectant solution, and then flash frozen in liquid nitrogen. The CryoLoops were put in vials and assembled on a crane for storage in liquid nitrogen until ready to diffract in the X-ray Crystallography Facility.

Results

The main research objectives were to improve anti-folate selectivity by exploring and comparing the unique binding properties of anti-folates against *Candida* and mammalian DHFR. In the fight against infectious diseases, information from crystal structures of huDHFR, CaDHFR, and CgDHFR can direct the future design of more potent and selective drug compounds. The anti-folates initially developed had used data gathered from crystal structures of CaDHFR and CgDHFR. However, the structure of huDHFR bound to these drug compounds was previously difficult to attain. Although UCP111E, the compound of interest in this project, demonstrated lower IC_{50} values (and therefore, greater selectivity) for the fungal species versus human, chemists still aimed for a redesign to further increase the differences between the indices. Therefore, solving structures of huDHFR bound to propargyl-linked anti-folates was a key step to attaining this goal. Greater selectivity of these drug compounds would not only increase the efficacy against fungal infections, but would also reduce toxicity in the human host.

The protein purification process involved affinity chromatography with a methotrexate column to isolate huDHFR. The lysed cell sample was added to the column, allowing for the binding of huDHFR to the beads containing methotrexate, a drug that impairs the formation of active tetrahydrofolate (THF) from inactive dihydrofolate (DHF) in the folate pathway. To elute huDHFR from the beads, DHF was added to the column, allowing the enzyme to preferentially

bind to DHF and to detach from methotrexate. Fractions containing huDHFR were confirmed through SDS-PAGE and gel electrophoresis. Purification of huDHFR resulting in 10 mg/L cultures yielded > 95% purity.

The first crystal tray (Figure 1 in Appendix A) contained very broad conditions to determine the most appropriate environment for crystal formation. Concentrations of lithium sulfate were 0.1 M, 0.15 M, and 0.2 M in rows A, B, and C respectively. PEG 4000 was at 20% (v/v), 25% (v/v), 30% (v/v), 35% (v/v), and 37% (v/v) in columns 1-5. In addition, 0.1 M Tris and 5% (v/v) ethanol remained constant in all wells. A protein concentration of 15 mg/mL was used, and the non-volatile additives were 1%, 3%, and 5% 1,8-diaminooctane in cavities I, II, and III, respectively. When comparing the three concentrations, nothing formed in 1% 1,8-diaminooctane, while 3% demonstrated phase separation and texture changes (seen as beige "oily" masses) and 5% revealed precipitation. Row B with 0.15 M lithium sulfate and column 3 with 30% (v/v) PEG 4000 showed the most phase separation, nucleation, and early signs of crystal formation; whereas, row A displayed more beige-colored masses of precipitate.

The second crystal tray (Figure 2 in Appendix A) used higher concentrations of 1,8-diaminooctane (i.e., 3%, 5%, and 7%), but the protein concentration remained 15 mg/mL. Lithium sulfate concentrations were changed to 0.1 M, 0.125 M, and 0.15 M; whereas, PEG 4000 concentrations of 18% (v/v), 20% (v/v), 22.5% (v/v), 25% (v/v), and 30% (v/v) were evaluated. Cavities I and II with 3% and 5% 1,8-diaminooctane, respectively, either showed no changes or demonstrated light to heavy precipitation with "oily" masses. This effect appeared most prominent in the first 3 columns with 18% (v/v), 20% (v/v) and 22.5% (v/v) PEG 4000, as well as in row A with 0.1 M lithium sulfate and row C with 0.15 M lithium sulfate. Cavity III with 7% 1,8-diaminooctane exhibited some crystal formation seen as thin "ice-like" plates in

columns 4 and 5 containing 25% and 30% (v/v) PEG 4000, respectively. Rows A, B, and C also displayed this result. In particular, B4 with 0.125 M lithium sulfate and 25% (v/v) PEG 4000 produced thin plates in cavities II and III.

Protein concentration was increased to 18 and 20 mg/mL in the third EasyXtal crystal tray (Figure 3 in Appendix A), as were concentrations of 1,8-diaminooctane to 5%, 7%, and 10%. PEG 4000 concentrations were carried over from the previous crystal tray, but lithium sulfate concentrations were changed to 0.125 M, 0.15 M, and 0.175 M. Crystal plate formation generally appeared in cavity III and rows A-C, with more prominent results in columns 4 and 5, similar to the previous tray. On the other hand, precipitation seen as small dark dots predominated cavity I with 5% 1,8-diaminooctane, especially in row A.

Further plans to optimize conditions included increasing 1,8-diaminooctane concentrations to 7%, 10%, and 13% in the fourth plate (Figure 4 in Appendix A) and to 10%, 15%, 20% in the fifth (Figure 5 in Appendix A). PEG 4000 at 25% (v/v), 27.5% (v/v), 30% (v/v), 32.5% (v/v), and 35% (v/v) were utilized in both trays. However, crystal tray #5 used 10% (v/v) ethanol, instead of 5% (v/v), and also required a stock of 2 M Tris buffer, rather than 1M, to accommodate the 500 μL volume limit for each well. Lithium sulfate concentrations between the third and fourth trays stayed the same, but this was increased to 0.2 M, 0.225 M, and 0.25 M for the fourth. Protein concentrations were 15 mg/mL.

Upon initial examination, cavity II with 10% 1,8-diaminooctane from crystal tray #4 consistently showed a mixture of precipitation and crystal formation seen as plates or striated rods in rows A-C. Cavity I containing 7% 1,8-diaminooctane also exhibited some crystals, but less so than in cavity II; whereas, cavity III with 13% 1,8-diaminooctane mostly revealed precipitation. A few weeks later though, single large plates appeared in B5, which previously had

no formations or just light precipitate. On the fifth tray, nearly all 3 cavities had crystal growth in the form of plates and needles, especially with the higher 1,8-diaminooctane concentrations. "Oily" formations were also mixed in with the crystals, particularly in columns 4 and 5 with 32.5% and 35% (v/v) PEG 4000, respectively.

In the sixth crystal tray (figure 6 in Appendix A), only lithium sulfate and PEG 4000 concentrations were changed in the reservoir solution. Rows A, B, and C had 0.25 M, 0.3 M, and 0.35 M lithium sulfate, respectively. Columns 1-5 had 25%, 27%, 29%, 31%, and 33% (v/v) PEG 4000. In addition, 10%, 15%, and 20% 1,8-diaminooctane were used. The concentration of huDHFR was 15 mg/mL. Row A mostly exhibited heavy, brown precipitation; however, rows B and C created noticeable crystals in all 3 cavities that were considered worthy of diffraction experiments. Crystals were gathered and flash-frozen in liquid nitrogen from C3 (0.1 M Tris, 0.35 M lithium sulfate, 29% (v/v) PEG 400, 10% (v/v) ethanol), C4 (0.1 M Tris, 0.35 M lithium sulfate, 31% (v/v) PEG 4000, 10% (v/v) ethanol), and C5 (0.1 M Tris, 0.35 M lithium sulfate, 33% (v/v) PEG 4000, 10% (v/v) ethanol).

Crystal tray #7 (figure 7 in Appendix A) used strontium chloride as the non-volatile additive in concentrations of 0.075 M, 0.1 M, and 0.125 M in cavities I, II, and III, respectively. Tris at 0.1 M and ethanol at 8% (v/v) remained constant in all wells. Lithium sulfate varied (0.33 M, 0.35 M, and 0.37 M) in the rows (A-C); PEG 4000 was 24% (v/v), 26.5 % (v/v), 29% (v/v), 31.5% (v/v), and 34% (v/v) in respective columns (1-5). Protein concentration was increased to 20 mg/mL. While all 3 rows formed tiny crystal, denser arrays of larger crystals appeared at higher PEG 4000 concentrations in columns 4 and 5 at 31.5% (v/v) and 34% (v/v), respectively. Higher concentrations of strontium chloride at 0.1 M and 0.125 M also created slightly larger crystals, particularly in rows A and B with 0.33 M and 0.35 M lithium sulfate, respectively. In

well B4 (0.1 M Tris, 0.35 M lithium sulfate, 31.5% (v/v) PEG 4000, 8.0% (v/v) ethanol), a hexagon-shaped crystal also appeared when the protein was exposed to 0.075 M strontium chloride. A foreign piece of fiber in the well may have also contributed to this phenomenon. In row C with 0.37 M lithium sulfate, 0.125 M strontium chloride produced larger crystals, but they were still too small for diffraction. Higher PEG concentrations in row C also revealed tannish-colored masses of precipitation.

Experimentation with different non-volatile additives continued into crystal tray #8 (figure 8 in Appendix A), which tested the effects of calcium chloride. Tris at 0.1 M and lithium sulfate at 0.35 M were kept constant in all wells. PEG 4000 as 24% (v/v), 26.5% (v/v), 29% (v/v), 31.5% (v/v), and 34% (v/v) were in columns 1-5; whereas, ethanol was 6% (v/v), 7% (v/v), and 8% (v/v) in rows A-C. HuDHFR concentrations of 11 mg/mL and 15 mg/mL were used, so cavity I contained 0.1 M calcium chloride with 11 mg/mL protein, cavity II had 0.1 M calcium chloride with 15 mg/mL protein, and cavity III, 0.15 M calcium chloride and 15 mg/mL protein. Crystals formed within three days; however, clumps of fused crystals, rather than individual ones, were mostly observed in each row. The crystallization process may have occurred too quickly, leading to crystal conglomerations in several wells, including C1 (0.1 M Tris, 0.35 M lithium sulfate, 24% (v/v) PEG 4000, 8% (v/v) ethanol). Nonetheless, some wells formed single, large rod-shaped crystals that were considered for diffraction (i.e., A4, B2, and B5).

The ninth plate (figure 9 in Appendix A) optimized the conditions from plate #7, with strontium chloride as the non-volatile additive. Rows contained 0.3 M, 0.35 M, and 0.37 M lithium sulfate, while PEG 4000 concentrations were broadened to 22% (v/v), 25% (v/v), 28% (v/v), 31.5% (v/v), and 34% (v/v) in the columns. Concentrations of huDHFR were 11 mg/mL and 15 mg/mL. Contents of individual cavities were as follows: 0.075 M strontium chloride and

11 mg/mL protein in I, 0.075 M strontium chloride and 15 mg/mL protein in II, and 0.125 M strontium chloride and 15 mg/mL protein in III. Heavy precipitation predominated in many wells, particularly those in row A. Although crystals did form, like in C1 (0.1 M Tris, 0.37 M lithium sulfate, 22% (v/v) PEG 4000, 8% (v/v) ethanol), precipitation was also present. The crystal sizes also did not differ from that in the seventh tray.

Consult Appendix A for images of specific cavities and wells for each crystal plate.

Discussion

For protein crystallization, adjustable parameters include the precipitant or additive concentration, pH, and temperature. As observed from the 1,8-diaminooctane plates in this project, higher concentrations of PEG 4000 and lithium sulfate in the reservoir solution generally had more successful crystal formations. Ethanol at 8 % (v/v) also seemed to work best, which is supported by previous experiments with huDHFR from K. Lamb.

The additive, 1,8-diaminooctane, produced crystals fairly quickly in about 1-2 weeks; however, the crystals were often very thin and fragile plates. Needles would form occasionally, but even those were difficult to harvest and freeze. As a result, other non-volatile additives were tested. Information from optimizing conditions in the 1,8-diaminooctane crystal trays (#1-6) were used to design additional trays. Known to produce more durable crystals, strontium chloride was plated for trays #7 and #9. The only caveat is that this additive takes about 4 weeks to produce results. The use of calcium chloride as different additive for tray #8 resulted in even more rapid crystal formation in a matter of days. Although certain conditions with calcium chloride created a few individual rods to form, several tended to fuse into larger clumps.

The aim of refining the crystallization conditions was to produce crystals of huDHFR/UCP111E suitable for diffraction studies. Despite the small, thin plate-like crystals initially seen in the 1,8-diaminooctane trays, a few larger ones (i.e., in B5 of tray #6) were seen after several more weeks flash-frozen in liquid nitrogen for diffraction. Hexagon-shaped crystals were also spotted in A5 and B1 of tray #7 with strontium chloride, but unfortunately, these were still too small. On the other hand, a sizable rod-shaped crystal was successfully collected for diffraction from B3 in tray #8 with calcium chloride. Attempts to shoot these potential crystals from 1,8-diaminooctane and calcium chloride in the X-ray crystallography facility yielded inadequate results. Based on the sparse and irregular diffraction patterns generated, these crystals likely contained salt, rather than protein.

In future experiments, 1,8-diaminooctane may be abandoned as a non-volatile additive, due to the fragility of the resultant crystals. Several attempts were already made to optimize conditions with this additive, so it may be best to experiment with others in subsequent trays. Given the structural similarities among the crystals developed from 1,8-diaminooctane, it could also be deduced that they were all just salt formations. Crystals from strontium chloride were not yet suitable for diffraction; nonetheless, preliminary results were promising. Future studies will focus on refining the crystallization conditions for this additive. Rather than applying similar crystallization conditions as 1,8-diaminooctane, broad parameters will be set and adjusted accordingly; a similar approach could be applied to calcium chloride. After all, there is little guarantee that any successful conditions from one additive would be applicable to another. Crystal structures of huDHFR, CaDHFR, and CgDHFR each bound to UCP111E would ideally be determined and compared separately to aid in the design of future anti-folate compounds.

Appendix A

Figure 1

Non-volatile additive: 1,8-diaminooctane

I: 1%
II: 3%
III: 5%

	1	2	3	4	5
A	[A1] 0.1 M Tris pH 7.5, **50.0 µl** 0.1 M Lithium sulfate, **25.0 µl** 20.0 %v/v PEG 4000, **200.0 µl** 5.0 %v/v Ethanol, **25.0 µl** Water, **200.0 µl**	[A2] 0.1 M Tris pH 7.5, **50.0 µl** 0.1 M Lithium sulfate, **25.0 µl** 25.0 %v/v PEG 4000, **250.0 µl** 5.0 %v/v Ethanol, **25.0 µl** Water, **150.0 µl**	[A3] 0.1 M Tris pH 7.5, **50.0 µl** 0.1 M Lithium sulfate, **25.0 µl** 30.0 %v/v PEG 4000, **300.0 µl** 5.0 %v/v Ethanol, **25.0 µl** Water, **100.0 µl**	[A4] 0.1 M Tris pH 7.5, **50.0 µl** 0.1 M Lithium sulfate, **25.0 µl** 35.0 %v/v PEG 4000, **350.0 µl** 5.0 %v/v Ethanol, **25.0 µl** Water, **50.0 µl**	[A5] 0.1 M Tris pH 7.5, **50.0 µl** 0.1 M Lithium sulfate, **25.0 µl** 37.0 %v/v PEG 4000, **370.0 µl** 5.0 %v/v Ethanol, **25.0 µl** Water, **30.0 µl**
B	[B1] 0.1 M Tris pH 7.5, **50.0 µl** 0.15 M Lithium sulfate, **37.5 µl** 20.0 %v/v PEG 4000, **200.0 µl** 5.0 %v/v Ethanol, **25.0 µl** Water, **187.5 µl**	[B2] 0.1 M Tris pH 7.5, **50.0 µl** 0.15 M Lithium sulfate, **37.5 µl** 25.0 %v/v PEG 4000, **250.0 µl** 5.0 %v/v Ethanol, **25.0 µl** Water, **137.5 µl**	[B3] 0.1 M Tris pH 7.5, **50.0 µl** 0.15 M Lithium sulfate, **37.5 µl** 30.0 %v/v PEG 4000, **300.0 µl** 5.0 %v/v Ethanol, **25.0 µl** Water, **87.5 µl**	[B4] 0.1 M Tris pH 7.5, **50.0 µl** 0.15 M Lithium sulfate, **37.5 µl** 35.0 %v/v PEG 4000, **350.0 µl** 5.0 %v/v Ethanol, **25.0 µl** Water, **37.5 µl**	[B5] 0.1 M Tris pH 7.5, **50.0 µl** 0.15 M Lithium sulfate, **37.5 µl** 37.0 %v/v PEG 4000, **370.0 µl** 5.0 %v/v Ethanol, **25.0 µl** Water, **17.5 µl**
C	[C1] 0.1 M Tris pH 7.5, **50.0 µl** 0.2 M Lithium sulfate, **50.0 µl** 20.0 %v/v PEG 4000, **200.0 µl** 5.0 %v/v Ethanol, **25.0 µl** Water, **175.0 µl**	[C2] 0.1 M Tris pH 7.5, **50.0 µl** 0.2 M Lithium sulfate, **50.0 µl** 25.0 %v/v PEG 4000, **250.0 µl** 5.0 %v/v Ethanol, **25.0 µl** Water, **125.0 µl**	[C3] 0.1 M Tris pH 7.5, **50.0 µl** 0.2 M Lithium sulfate, **50.0 µl** 30.0 %v/v PEG 4000, **300.0 µl** 5.0 %v/v Ethanol, **25.0 µl** Water, **75.0 µl**	[C4] 0.1 M Tris pH 7.5, **50.0 µl** 0.2 M Lithium sulfate, **50.0 µl** 35.0 %v/v PEG 4000, **350.0 µl** 5.0 %v/v Ethanol, **25.0 µl** Water, **25.0 µl**	[C5] 0.1 M Tris pH 7.5, **50.0 µl** 0.2 M Lithium sulfate, **50.0 µl** 37.0 %v/v PEG 4000, **370.0 µl** 5.0 %v/v Ethanol, **25.0 µl** Water, **5.0 µl**

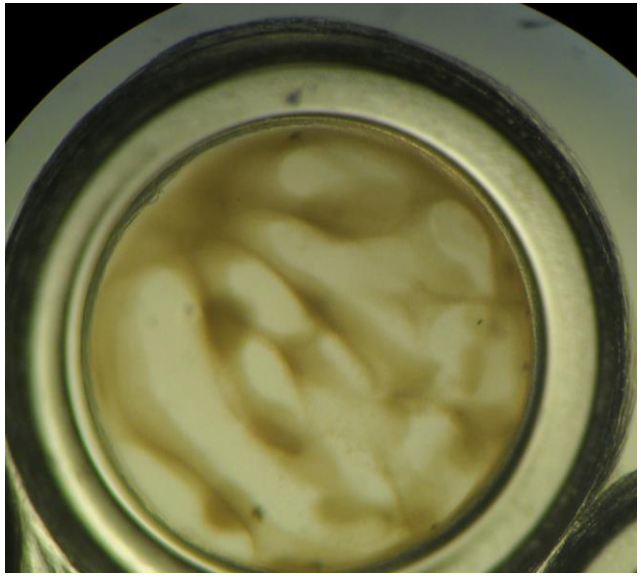

A4, II

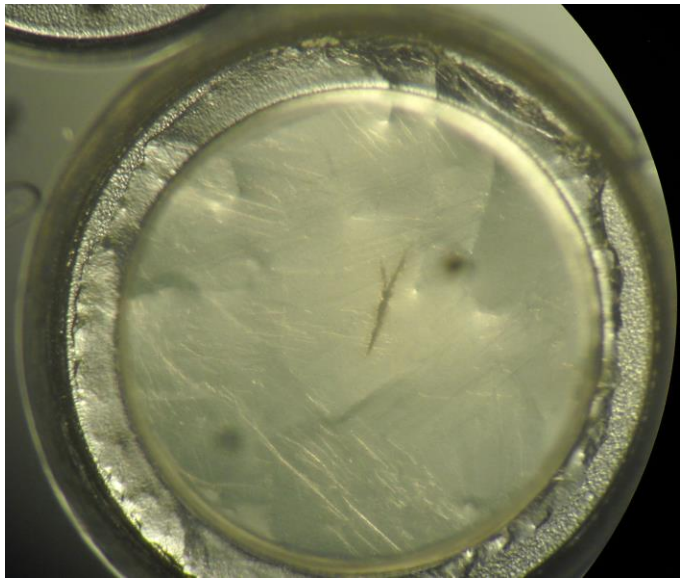

B1, III

Figure 2

Non-volatile additive: 1,8-diaminooctane

I: 3%
II: 5%
III: 7%

	1	2	3	4	5
A	[A1] 0.1 M Tris pH 7.5, **50.0 µl** 0.1 M Lithium Sulfate, **25.0 µl** 18.0 %v/v PEG 4000, **180.0 µl** 5.0 %v/v Ethanol, **25.0 µl** Water, **220.0 µl**	[A2] 0.1 M Tris pH 7.5, **50.0 µl** 0.1 M Lithium Sulfate, **25.0 µl** 20.0 %v/v PEG 4000, **200.0 µl** 5.0 %v/v Ethanol, **25.0 µl** Water, **200.0 µl**	[A3] 0.1 M Tris pH 7.5, **50.0 µl** 0.1 M Lithium Sulfate, **25.0 µl** 22.5 %v/v PEG 4000, **225.0 µl** 5.0 %v/v Ethanol, **25.0 µl** Water, **175.0 µl**	[A4] 0.1 M Tris pH 7.5, **50.0 µl** 0.1 M Lithium Sulfate, **25.0 µl** 25.0 %v/v PEG 4000, **250.0 µl** 5.0 %v/v Ethanol, **25.0 µl** Water, **150.0 µl**	[A5] 0.1 M Tris pH 7.5, **50.0 µl** 0.1 M Lithium Sulfate, **25.0 µl** 30.0 %v/v PEG 4000, **300.0 µl** 5.0 %v/v Ethanol, **25.0 µl** Water, **100.0 µl**
B	[B1] 0.1 M Tris pH 7.5, **50.0 µl** 0.125 M Lithium Sulfate, **31.3 µl** 18.0 %v/v PEG 4000, **180.0 µl** 5.0 %v/v Ethanol, **25.0 µl** Water, **213.7 µl**	[B2] 0.1 M Tris pH 7.5, **50.0 µl** 0.125 M Lithium Sulfate, **31.3 µl** 20.0 %v/v PEG 4000, **200.0 µl** 5.0 %v/v Ethanol, **25.0 µl** Water, **193.7 µl**	[B3] 0.1 M Tris pH 7.5, **50.0 µl** 0.125 M Lithium Sulfate, **31.3 µl** 22.5 %v/v PEG 4000, **225.0 µl** 5.0 %v/v Ethanol, **25.0 µl** Water, **168.7 µl**	[B4] 0.1 M Tris pH 7.5, **50.0 µl** 0.125 M Lithium Sulfate, **31.3 µl** 25.0 %v/v PEG 4000, **250.0 µl** 5.0 %v/v Ethanol, **25.0 µl** Water, **143.7 µl**	[B5] 0.1 M Tris pH 7.5, **50.0 µl** 0.125 M Lithium Sulfate, **31.3 µl** 30.0 %v/v PEG 4000, **300.0 µl** 5.0 %v/v Ethanol, **25.0 µl** Water, **93.7 µl**
C	[C1] 0.1 M Tris pH 7.5, **50.0 µl** 0.15 M Lithium Sulfate, **37.5 µl** 18.0 %v/v PEG 4000, **180.0 µl** 5.0 %v/v Ethanol, **25.0 µl** Water, **207.5 µl**	[C2] 0.1 M Tris pH 7.5, **50.0 µl** 0.15 M Lithium Sulfate, **37.5 µl** 20.0 %v/v PEG 4000, **200.0 µl** 5.0 %v/v Ethanol, **25.0 µl** Water, **187.5 µl**	[C3] 0.1 M Tris pH 7.5, **50.0 µl** 0.15 M Lithium Sulfate, **37.5 µl** 22.5 %v/v PEG 4000, **225.0 µl** 5.0 %v/v Ethanol, **25.0 µl** Water, **162.5 µl**	[C4] 0.1 M Tris pH 7.5, **50.0 µl** 0.15 M Lithium Sulfate, **37.5 µl** 25.0 %v/v PEG 4000, **250.0 µl** 5.0 %v/v Ethanol, **25.0 µl** Water, **137.5 µl**	[C5] 0.1 M Tris pH 7.5, **50.0 µl** 0.15 M Lithium Sulfate, **37.5 µl** 30.0 %v/v PEG 4000, **300.0 µl** 5.0 %v/v Ethanol, **25.0 µl** Water, **87.5 µl**

B4, III

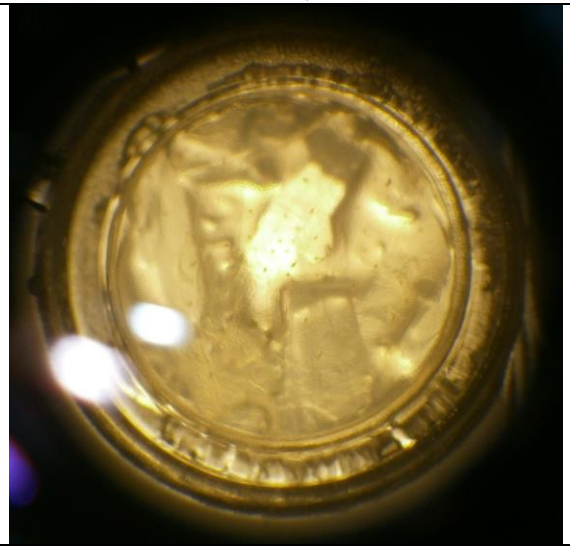

C5, III

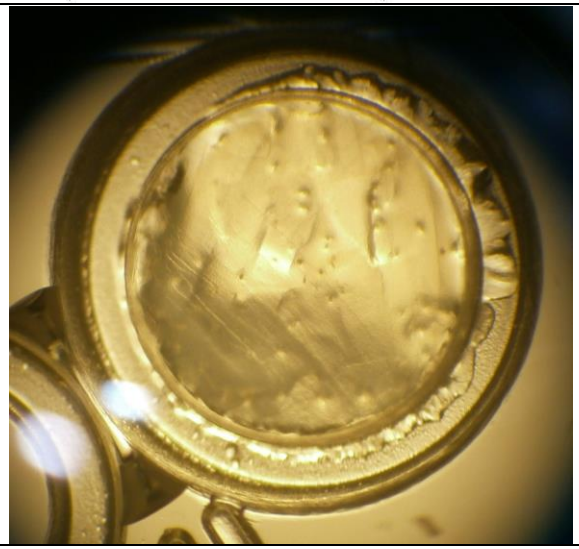

Figure 3

Non-volatile additive: 1,8-diaminooctane

I: 5%
II: 7%
III: 10%

	1	2	3	4	5
A	[A1] 0.1 M Tris pH 7.5, **75.0 µl** 0.1 M Lithium sulfate, **37.5 µl** 18.0 %v/v PEG 4000, **270.0 µl** 5.0 %v/v Ethanol, **37.5 µl** Water, **330.0 µl**	[A2] 0.1 M Tris pH 7.5, **75.0 µl** 0.1 M Lithium sulfate, **37.5 µl** 20.0 %v/v PEG 4000, **300.0 µl** 5.0 %v/v Ethanol, **37.5 µl** Water, **300.0 µl**	[A3] 0.1 M Tris pH 7.5, **75.0 µl** 0.1 M Lithium sulfate, **37.5 µl** 22.5 %v/v PEG 4000, **337.5 µl** 5.0 %v/v Ethanol, **37.5 µl** Water, **262.5 µl**	[A4] 0.1 M Tris pH 7.5, **75.0 µl** 0.1 M Lithium sulfate, **37.5 µl** 25.0 %v/v PEG 4000, **375.0 µl** 5.0 %v/v Ethanol, **37.5 µl** Water, **225.0 µl**	[A5] 0.1 M Tris pH 7.5, **75.0 µl** 0.1 M Lithium sulfate, **37.5 µl** 30.0 %v/v PEG 4000, **450.0 µl** 5.0 %v/v Ethanol, **37.5 µl** Water, **150.0 µl**
B	[B1] 0.1 M Tris pH 7.5, **75.0 µl** 0.125 M Lithium sulfate, **46.9 µl** 18.0 %v/v PEG 4000, **270.0 µl** 5.0 %v/v Ethanol, **37.5 µl** Water, **320.6 µl**	[B2] 0.1 M Tris pH 7.5, **75.0 µl** 0.125 M Lithium sulfate, **46.9 µl** 20.0 %v/v PEG 4000, **300.0 µl** 5.0 %v/v Ethanol, **37.5 µl** Water, **290.6 µl**	[B3] 0.1 M Tris pH 7.5, **75.0 µl** 0.125 M Lithium sulfate, **46.9 µl** 22.5 %v/v PEG 4000, **337.5 µl** 5.0 %v/v Ethanol, **37.5 µl** Water, **253.1 µl**	[B4] 0.1 M Tris pH 7.5, **75.0 µl** 0.125 M Lithium sulfate, **46.9 µl** 25.0 %v/v PEG 4000, **375.0 µl** 5.0 %v/v Ethanol, **37.5 µl** Water, **215.6 µl**	[B5] 0.1 M Tris pH 7.5, **75.0 µl** 0.125 M Lithium sulfate, **46.9 µl** 30.0 %v/v PEG 4000, **450.0 µl** 5.0 %v/v Ethanol, **37.5 µl** Water, **140.6 µl**
C	[C1] 0.1 M Tris pH 7.5, **75.0 µl** 0.15 M Lithium sulfate, **56.3 µl** 18.0 %v/v PEG 4000, **270.0 µl** 5.0 %v/v Ethanol, **37.5 µl** Water, **311.2 µl**	[C2] 0.1 M Tris pH 7.5, **75.0 µl** 0.15 M Lithium sulfate, **56.3 µl** 20.0 %v/v PEG 4000, **300.0 µl** 5.0 %v/v Ethanol, **37.5 µl** Water, **281.2 µl**	[C3] 0.1 M Tris pH 7.5, **75.0 µl** 0.15 M Lithium sulfate, **56.3 µl** 22.5 %v/v PEG 4000, **337.5 µl** 5.0 %v/v Ethanol, **37.5 µl** Water, **243.7 µl**	[C4] 0.1 M Tris pH 7.5, **75.0 µl** 0.15 M Lithium sulfate, **56.3 µl** 25.0 %v/v PEG 4000, **375.0 µl** 5.0 %v/v Ethanol, **37.5 µl** Water, **206.2 µl**	[C5] 0.1 M Tris pH 7.5, **75.0 µl** 0.15 M Lithium sulfate, **56.3 µl** 30.0 %v/v PEG 4000, **450.0 µl** 5.0 %v/v Ethanol, **37.5 µl** Water, **131.2 µl**

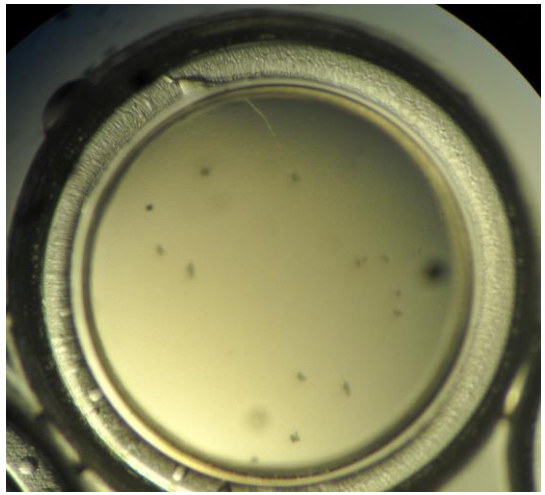

A4, I

B5, III

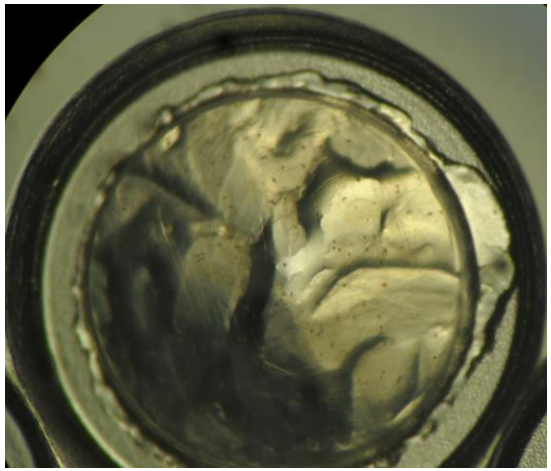

C1, II

Figure 4

Non-volatile additive: 1,8-diaminooctane

I: 7%
II: 10%
III: 13%

	1	2	3	4	5
A	[A1] 0.1 M Tris pH 7.5, **50.0 µl** 0.125 M Lithium sulfate, **31.3 µl** 18.0 %v/v PEG 4000, **180.0 µl** 5.0 %v/v Ethanol, **25.0 µl** Water, **213.7 µl**	[A2] 0.1 M Tris pH 7.5, **50.0 µl** 0.125 M Lithium sulfate, **31.3 µl** 20.0 %v/v PEG 4000, **200.0 µl** 5.0 %v/v Ethanol, **25.0 µl** Water, **193.7 µl**	[A3] 0.1 M Tris pH 7.5, **50.0 µl** 0.125 M Lithium sulfate, **31.3 µl** 22.5 %v/v PEG 4000, **225.0 µl** 5.0 %v/v Ethanol, **25.0 µl** Water, **168.7 µl**	[A4] 0.1 M Tris pH 7.5, **50.0 µl** 0.125 M Lithium sulfate, **31.3 µl** 25.0 %v/v PEG 4000, **250.0 µl** 5.0 %v/v Ethanol, **25.0 µl** Water, **143.7 µl**	[A5] 0.1 M Tris pH 7.5, **50.0 µl** 0.125 M Lithium sulfate, **31.3 µl** 30.0 %v/v PEG 4000, **300.0 µl** 5.0 %v/v Ethanol, **25.0 µl** Water, **93.7 µl**
B	[B1] 0.1 M Tris pH 7.5, **50.0 µl** 0.15 M Lithium sulfate, **37.5 µl** 18.0 %v/v PEG 4000, **180.0 µl** 5.0 %v/v Ethanol, **25.0 µl** Water, **207.5 µl**	[B2] 0.1 M Tris pH 7.5, **50.0 µl** 0.15 M Lithium sulfate, **37.5 µl** 20.0 %v/v PEG 4000, **200.0 µl** 5.0 %v/v Ethanol, **25.0 µl** Water, **187.5 µl**	[B3] 0.1 M Tris pH 7.5, **50.0 µl** 0.15 M Lithium sulfate, **37.5 µl** 22.5 %v/v PEG 4000, **225.0 µl** 5.0 %v/v Ethanol, **25.0 µl** Water, **162.5 µl**	[B4] 0.1 M Tris pH 7.5, **50.0 µl** 0.15 M Lithium sulfate, **37.5 µl** 25.0 %v/v PEG 4000, **250.0 µl** 5.0 %v/v Ethanol, **25.0 µl** Water, **137.5 µl**	[B5] 0.1 M Tris pH 7.5, **50.0 µl** 0.15 M Lithium sulfate, **37.5 µl** 30.0 %v/v PEG 4000, **300.0 µl** 5.0 %v/v Ethanol, **25.0 µl** Water, **87.5 µl**
C	[C1] 0.1 M Tris pH 7.5, **50.0 µl** 0.175 M Lithium sulfate, **43.8 µl** 18.0 %v/v PEG 4000, **180.0 µl** 5.0 %v/v Ethanol, **25.0 µl** Water, **201.2 µl**	[C2] 0.1 M Tris pH 7.5, **50.0 µl** 0.175 M Lithium sulfate, **43.8 µl** 20.0 %v/v PEG 4000, **200.0 µl** 5.0 %v/v Ethanol, **25.0 µl** Water, **181.2 µl**	[C3] 0.1 M Tris pH 7.5, **50.0 µl** 0.175 M Lithium sulfate, **43.8 µl** 22.5 %v/v PEG 4000, **225.0 µl** 5.0 %v/v Ethanol, **25.0 µl** Water, **156.2 µl**	[C4] 0.1 M Tris pH 7.5, **50.0 µl** 0.175 M Lithium sulfate, **43.8 µl** 25.0 %v/v PEG 4000, **250.0 µl** 5.0 %v/v Ethanol, **25.0 µl** Water, **131.2 µl**	[C5] 0.1 M Tris pH 7.5, **50.0 µl** 0.175 M Lithium sulfate, **43.8 µl** 30.0 %v/v PEG 4000, **300.0 µl** 5.0 %v/v Ethanol, **25.0 µl** Water, **81.2 µl**

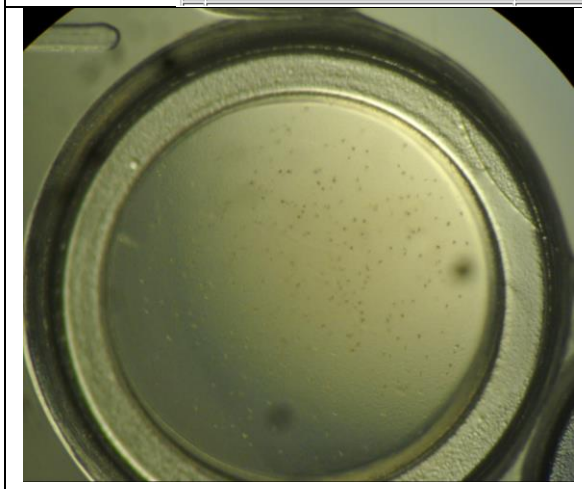

C1, III

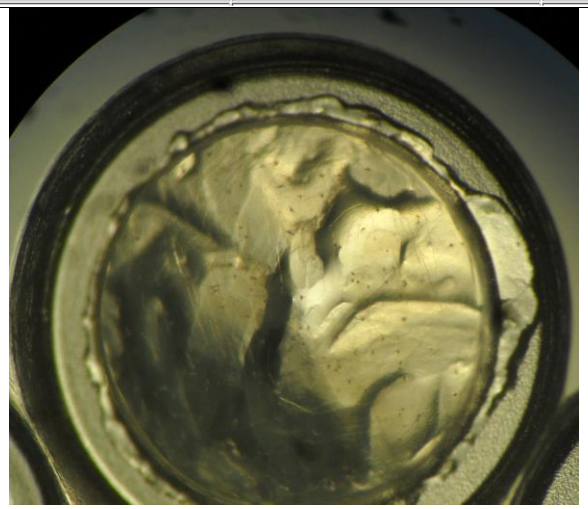

B3, I

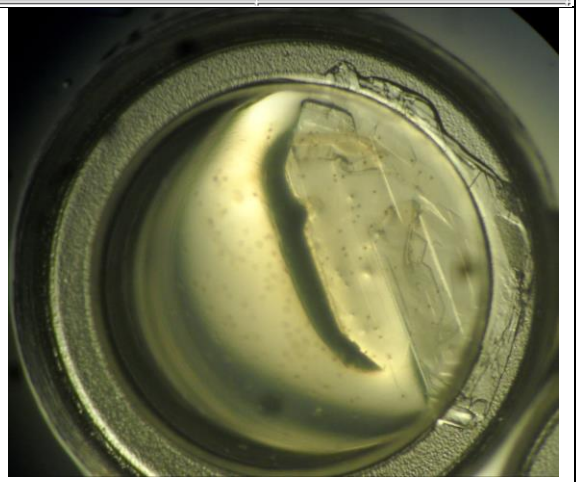

B5, II

Figure 5

Non-volatile additive: 1,8-diaminooctane

I: 10%
II: 15%
III: 20%

	1	2	3	4	5
A	[A1] 0.1 M Tris pH 7.5, **25.0 µl** 0.2 M Lithium Sulfate, **50.0 µl** 25.0 %v/v PEG 4000, **250.0 µl** 10.0 %v/v Ethanol, **50.0 µl** Water, **125.0 µl**	[A2] 0.1 M Tris pH 7.5, **25.0 µl** 0.2 M Lithium Sulfate, **50.0 µl** 27.5 %v/v PEG 4000, **275.0 µl** 10.0 %v/v Ethanol, **50.0 µl** Water, **100.0 µl**	[A3] 0.1 M Tris pH 7.5, **25.0 µl** 0.2 M Lithium Sulfate, **50.0 µl** 30.0 %v/v PEG 4000, **300.0 µl** 10.0 %v/v Ethanol, **50.0 µl** Water, **75.0 µl**	[A4] 0.1 M Tris pH 7.5, **25.0 µl** 0.2 M Lithium Sulfate, **50.0 µl** 32.5 %v/v PEG 4000, **325.0 µl** 10.0 %v/v Ethanol, **50.0 µl** Water, **50.0 µl**	[A5] 0.1 M Tris pH 7.5, **25.0 µl** 0.2 M Lithium Sulfate, **50.0 µl** 35.0 %v/v PEG 4000, **350.0 µl** 10.0 %v/v Ethanol, **50.0 µl** Water, **25.0 µl**
B	[B1] 0.1 M Tris pH 7.5, **25.0 µl** 0.225 M Lithium Sulfate, **56.3 µl** 25.0 %v/v PEG 4000, **250.0 µl** 10.0 %v/v Ethanol, **50.0 µl** Water, **118.7 µl**	[B2] 0.1 M Tris pH 7.5, **25.0 µl** 0.225 M Lithium Sulfate, **56.3 µl** 27.5 %v/v PEG 4000, **275.0 µl** 10.0 %v/v Ethanol, **50.0 µl** Water, **93.7 µl**	[B3] 0.1 M Tris pH 7.5, **25.0 µl** 0.225 M Lithium Sulfate, **56.3 µl** 30.0 %v/v PEG 4000, **300.0 µl** 10.0 %v/v Ethanol, **50.0 µl** Water, **68.7 µl**	[B4] 0.1 M Tris pH 7.5, **25.0 µl** 0.225 M Lithium Sulfate, **56.3 µl** 32.5 %v/v PEG 4000, **325.0 µl** 10.0 %v/v Ethanol, **50.0 µl** Water, **43.7 µl**	[B5] 0.1 M Tris pH 7.5, **25.0 µl** 0.225 M Lithium Sulfate, **56.3 µl** 35.0 %v/v PEG 4000, **350.0 µl** 10.0 %v/v Ethanol, **50.0 µl** Water, **18.7 µl**
C	[C1] 0.1 M Tris pH 7.5, **25.0 µl** 0.25 M Lithium Sulfate, **62.5 µl** 25.0 %v/v PEG 4000, **250.0 µl** 10.0 %v/v Ethanol, **50.0 µl** Water, **112.5 µl**	[C2] 0.1 M Tris pH 7.5, **25.0 µl** 0.25 M Lithium Sulfate, **62.5 µl** 27.5 %v/v PEG 4000, **275.0 µl** 10.0 %v/v Ethanol, **50.0 µl** Water, **87.5 µl**	[C3] 0.1 M Tris pH 7.5, **25.0 µl** 0.25 M Lithium Sulfate, **62.5 µl** 30.0 %v/v PEG 4000, **300.0 µl** 10.0 %v/v Ethanol, **50.0 µl** Water, **62.5 µl**	[C4] 0.1 M Tris pH 7.5, **25.0 µl** 0.25 M Lithium Sulfate, **62.5 µl** 32.5 %v/v PEG 4000, **325.0 µl** 10.0 %v/v Ethanol, **50.0 µl** Water, **37.5 µl**	[C5] 0.1 M Tris pH 7.5, **25.0 µl** 0.25 M Lithium Sulfate, **62.5 µl** 35.0 %v/v PEG 4000, **350.0 µl** 10.0 %v/v Ethanol, **50.0 µl** Water, **12.5 µl**

B2, II

C4, III

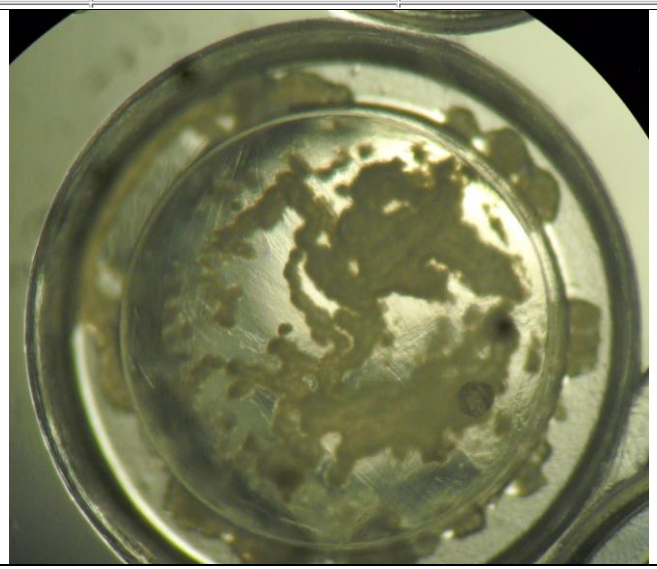

Figure 6

Non-volatile additive: 1,8-diaminooctane

I: 10%
II: 15%
III: 20%

	1	2	3	4	5
A	[A1] 0.1 M Tris pH 7.5, **25.0 µl** 0.25 M Lithium Sulfate, **62.5 µl** 25.0 %v/v PEG 4000, **250.0 µl** 10.0 %v/v Ethanol, **50.0 µl** Water, **112.5 µl**	[A2] 0.1 M Tris pH 7.5, **25.0 µl** 0.25 M Lithium Sulfate, **62.5 µl** 27.0 %v/v PEG 4000, **270.0 µl** 10.0 %v/v Ethanol, **50.0 µl** Water, **92.5 µl**	[A3] 0.1 M Tris pH 7.5, **25.0 µl** 0.25 M Lithium Sulfate, **62.5 µl** 29.0 %v/v PEG 4000, **290.0 µl** 10.0 %v/v Ethanol, **50.0 µl** Water, **72.5 µl**	[A4] 0.1 M Tris pH 7.5, **25.0 µl** 0.25 M Lithium Sulfate, **62.5 µl** 31.0 %v/v PEG 4000, **310.0 µl** 10.0 %v/v Ethanol, **50.0 µl** Water, **52.5 µl**	[A5] 0.1 M Tris pH 7.5, **25.0 µl** 0.25 M Lithium Sulfate, **62.5 µl** 33.0 %v/v PEG 4000, **330.0 µl** 10.0 %v/v Ethanol, **50.0 µl** Water, **32.5 µl**
B	[B1] 0.1 M Tris pH 7.5, **25.0 µl** 0.3 M Lithium Sulfate, **75.0 µl** 25.0 %v/v PEG 4000, **250.0 µl** 10.0 %v/v Ethanol, **50.0 µl** Water, **100.0 µl**	[B2] 0.1 M Tris pH 7.5, **25.0 µl** 0.3 M Lithium Sulfate, **75.0 µl** 27.0 %v/v PEG 4000, **270.0 µl** 10.0 %v/v Ethanol, **50.0 µl** Water, **80.0 µl**	[B3] 0.1 M Tris pH 7.5, **25.0 µl** 0.3 M Lithium Sulfate, **75.0 µl** 29.0 %v/v PEG 4000, **290.0 µl** 10.0 %v/v Ethanol, **50.0 µl** Water, **60.0 µl**	[B4] 0.1 M Tris pH 7.5, **25.0 µl** 0.3 M Lithium Sulfate, **75.0 µl** 31.0 %v/v PEG 4000, **310.0 µl** 10.0 %v/v Ethanol, **50.0 µl** Water, **40.0 µl**	[B5] 0.1 M Tris pH 7.5, **25.0 µl** 0.3 M Lithium Sulfate, **75.0 µl** 33.0 %v/v PEG 4000, **330.0 µl** 10.0 %v/v Ethanol, **50.0 µl** Water, **20.0 µl**
C	[C1] 0.1 M Tris pH 7.5, **25.0 µl** 0.35 M Lithium Sulfate, **87.5 µl** 25.0 %v/v PEG 4000, **250.0 µl** 10.0 %v/v Ethanol, **50.0 µl** Water, **87.5 µl**	[C2] 0.1 M Tris pH 7.5, **25.0 µl** 0.35 M Lithium Sulfate, **87.5 µl** 27.0 %v/v PEG 4000, **270.0 µl** 10.0 %v/v Ethanol, **50.0 µl** Water, **67.5 µl**	[C3] 0.1 M Tris pH 7.5, **25.0 µl** 0.35 M Lithium Sulfate, **87.5 µl** 29.0 %v/v PEG 4000, **290.0 µl** 10.0 %v/v Ethanol, **50.0 µl** Water, **47.5 µl**	[C4] 0.1 M Tris pH 7.5, **25.0 µl** 0.35 M Lithium Sulfate, **87.5 µl** 31.0 %v/v PEG 4000, **310.0 µl** 10.0 %v/v Ethanol, **50.0 µl** Water, **27.5 µl**	[C5] 0.1 M Tris pH 7.5, **25.0 µl** 0.35 M Lithium Sulfate, **87.5 µl** 33.0 %v/v PEG 4000, **330.0 µl** 10.0 %v/v Ethanol, **50.0 µl** Water, **7.5 µl**

B5, II

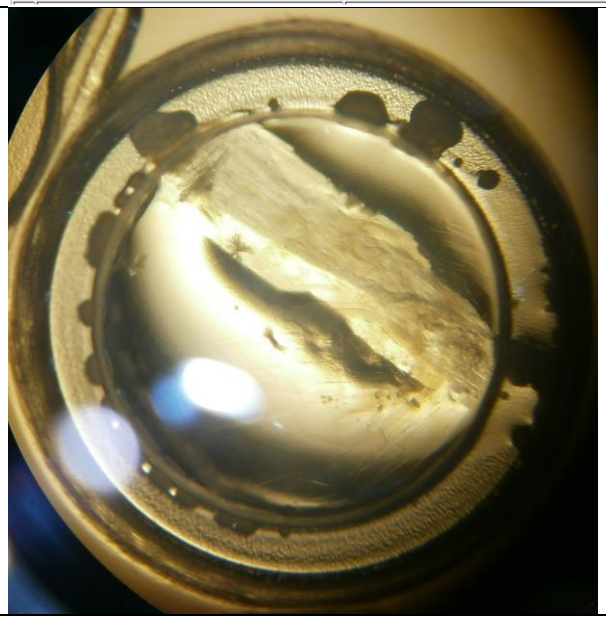

C3, III

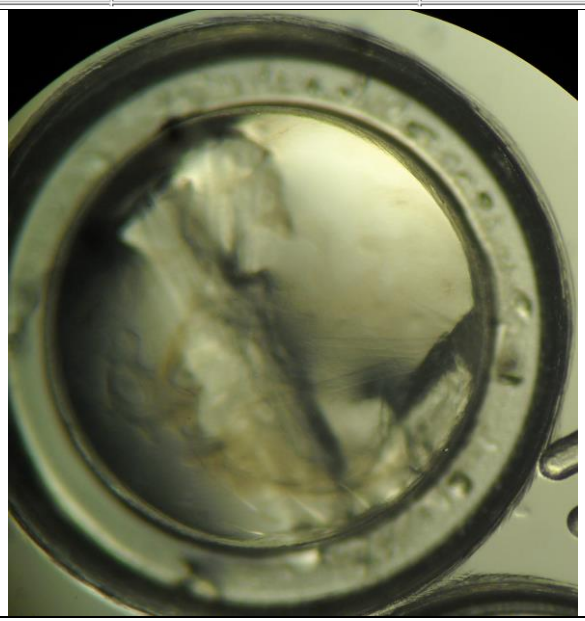

Figure 7

Non-volatile additive: Strontium Chloride

I: 0.075 M
II: 0.1 M
III: 0.125 M

	1	2	3	4	5
A	[A1] 0.1 M Tris pH 7.5, **25.0 µl** 0.33 M Lithium Sulfate, **82.5 µl** 24.0 %v/v PEG 4000, **240.0 µl** 8.0 %v/v Ethanol, **40.0 µl** Water, **112.5 µl**	[A2] 0.1 M Tris pH 7.5, **25.0 µl** 0.33 M Lithium Sulfate, **82.5 µl** 26.5 %v/v PEG 4000, **265.0 µl** 8.0 %v/v Ethanol, **40.0 µl** Water, **87.5 µl**	[A3] 0.1 M Tris pH 7.5, **25.0 µl** 0.33 M Lithium Sulfate, **82.5 µl** 29.0 %v/v PEG 4000, **290.0 µl** 8.0 %v/v Ethanol, **40.0 µl** Water, **62.5 µl**	[A4] 0.1 M Tris pH 7.5, **25.0 µl** 0.33 M Lithium Sulfate, **82.5 µl** 31.5 %v/v PEG 4000, **315.0 µl** 8.0 %v/v Ethanol, **40.0 µl** Water, **37.5 µl**	[A5] 0.1 M Tris pH 7.5, **25.0 µl** 0.33 M Lithium Sulfate, **82.5 µl** 34.0 %v/v PEG 4000, **340.0 µl** 8.0 %v/v Ethanol, **40.0 µl** Water, **12.5 µl**
B	[B1] 0.1 M Tris pH 7.5, **25.0 µl** 0.35 M Lithium Sulfate, **87.5 µl** 24.0 %v/v PEG 4000, **240.0 µl** 8.0 %v/v Ethanol, **40.0 µl** Water, **107.5 µl**	[B2] 0.1 M Tris pH 7.5, **25.0 µl** 0.35 M Lithium Sulfate, **87.5 µl** 26.5 %v/v PEG 4000, **265.0 µl** 8.0 %v/v Ethanol, **40.0 µl** Water, **82.5 µl**	[B3] 0.1 M Tris pH 7.5, **25.0 µl** 0.35 M Lithium Sulfate, **87.5 µl** 29.0 %v/v PEG 4000, **290.0 µl** 8.0 %v/v Ethanol, **40.0 µl** Water, **57.5 µl**	[B4] 0.1 M Tris pH 7.5, **25.0 µl** 0.35 M Lithium Sulfate, **87.5 µl** 31.5 %v/v PEG 4000, **315.0 µl** 8.0 %v/v Ethanol, **40.0 µl** Water, **32.5 µl**	[B5] 0.1 M Tris pH 7.5, **25.0 µl** 0.35 M Lithium Sulfate, **87.5 µl** 34.0 %v/v PEG 4000, **340.0 µl** 8.0 %v/v Ethanol, **40.0 µl** Water, **7.5 µl**
C	[C1] 0.1 M Tris pH 7.5, **25.0 µl** 0.37 M Lithium Sulfate, **92.5 µl** 24.0 %v/v PEG 4000, **240.0 µl** 8.0 %v/v Ethanol, **40.0 µl** Water, **102.5 µl**	[C2] 0.1 M Tris pH 7.5, **25.0 µl** 0.37 M Lithium Sulfate, **92.5 µl** 26.5 %v/v PEG 4000, **265.0 µl** 8.0 %v/v Ethanol, **40.0 µl** Water, **77.5 µl**	[C3] 0.1 M Tris pH 7.5, **25.0 µl** 0.37 M Lithium Sulfate, **92.5 µl** 29.0 %v/v PEG 4000, **290.0 µl** 8.0 %v/v Ethanol, **40.0 µl** Water, **52.5 µl**	[C4] 0.1 M Tris pH 7.5, **25.0 µl** 0.37 M Lithium Sulfate, **92.5 µl** 31.5 %v/v PEG 4000, **315.0 µl** 8.0 %v/v Ethanol, **40.0 µl** Water, **27.5 µl**	[C5] 0.1 M Tris pH 7.5, **25.0 µl** 0.37 M Lithium Sulfate, **92.5 µl** 34.0 %v/v PEG 4000, **340.0 µl** 8.0 %v/v Ethanol, **40.0 µl** Water, **2.5 µl**

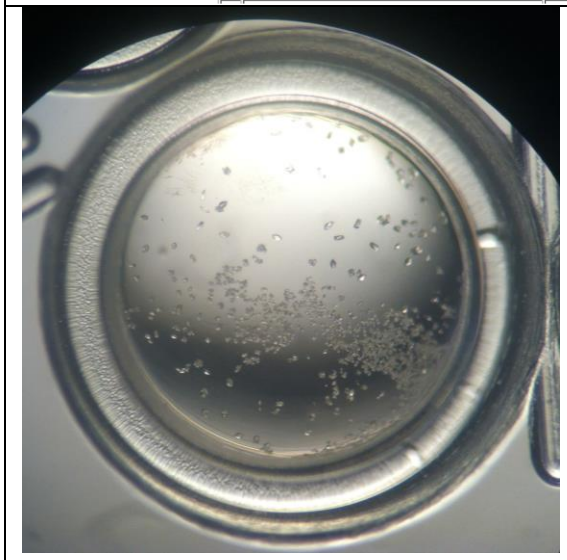

A3, III

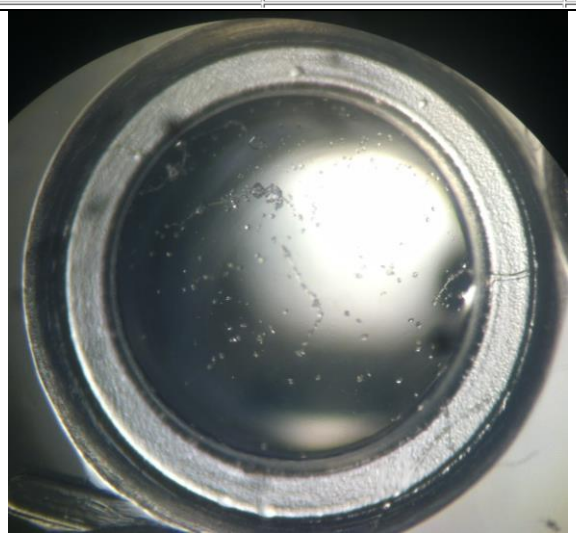

B4, I

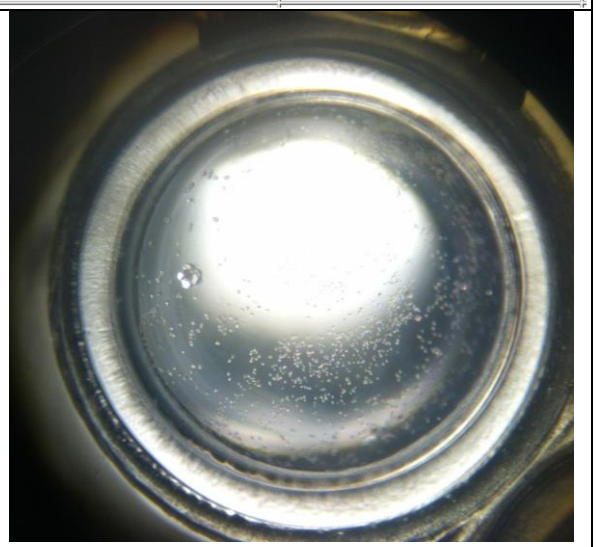

C4, II

Figure 8

Non-volatile additive: Calcium Chloride

I: 0.1 M
II: 0.1 M
III: 0.15 M

	1	2	3	4	5
A	[A1] 0.1 M Tris pH 7.5, **25.0 µl** 0.35 M Lithium Sulfate, **87.5 µl** 24.0 %v/v PEG 4000, **240.0 µl** 6.0 %v/v Ethanol, **30.0 µl** Water, **117.5 µl**	[A2] 0.1 M Tris pH 7.5, **25.0 µl** 0.35 M Lithium Sulfate, **87.5 µl** 26.5 %v/v PEG 4000, **265.0 µl** 6.0 %v/v Ethanol, **30.0 µl** Water, **92.5 µl**	[A3] 0.1 M Tris pH 7.5, **25.0 µl** 0.35 M Lithium Sulfate, **87.5 µl** 29.0 %v/v PEG 4000, **290.0 µl** 6.0 %v/v Ethanol, **30.0 µl** Water, **67.5 µl**	[A4] 0.1 M Tris pH 7.5, **25.0 µl** 0.35 M Lithium Sulfate, **87.5 µl** 31.5 %v/v PEG 4000, **315.0 µl** 6.0 %v/v Ethanol, **30.0 µl** Water, **42.5 µl**	[A5] 0.1 M Tris pH 7.5, **25.0 µl** 0.35 M Lithium Sulfate, **87.5 µl** 34.0 %v/v PEG 4000, **340.0 µl** 6.0 %v/v Ethanol, **30.0 µl** Water, **17.5 µl**
B	[B1] 0.1 M Tris pH 7.5, **25.0 µl** 0.35 M Lithium Sulfate, **87.5 µl** 24.0 %v/v PEG 4000, **240.0 µl** 7.0 %v/v Ethanol, **35.0 µl** Water, **112.5 µl**	[B2] 0.1 M Tris pH 7.5, **25.0 µl** 0.35 M Lithium Sulfate, **87.5 µl** 26.5 %v/v PEG 4000, **265.0 µl** 7.0 %v/v Ethanol, **35.0 µl** Water, **87.5 µl**	[B3] 0.1 M Tris pH 7.5, **25.0 µl** 0.35 M Lithium Sulfate, **87.5 µl** 29.0 %v/v PEG 4000, **290.0 µl** 7.0 %v/v Ethanol, **35.0 µl** Water, **62.5 µl**	[B4] 0.1 M Tris pH 7.5, **25.0 µl** 0.35 M Lithium Sulfate, **87.5 µl** 31.5 %v/v PEG 4000, **315.0 µl** 7.0 %v/v Ethanol, **35.0 µl** Water, **37.5 µl**	[B5] 0.1 M Tris pH 7.5, **25.0 µl** 0.35 M Lithium Sulfate, **87.5 µl** 34.0 %v/v PEG 4000, **340.0 µl** 7.0 %v/v Ethanol, **35.0 µl** Water, **12.5 µl**
C	[C1] 0.1 M Tris pH 7.5, **25.0 µl** 0.35 M Lithium Sulfate, **87.5 µl** 24.0 %v/v PEG 4000, **240.0 µl** 8.0 %v/v Ethanol, **40.0 µl** Water, **107.5 µl**	[C2] 0.1 M Tris pH 7.5, **25.0 µl** 0.35 M Lithium Sulfate, **87.5 µl** 26.5 %v/v PEG 4000, **265.0 µl** 8.0 %v/v Ethanol, **40.0 µl** Water, **82.5 µl**	[C3] 0.1 M Tris pH 7.5, **25.0 µl** 0.35 M Lithium Sulfate, **87.5 µl** 29.0 %v/v PEG 4000, **290.0 µl** 8.0 %v/v Ethanol, **40.0 µl** Water, **57.5 µl**	[C4] 0.1 M Tris pH 7.5, **25.0 µl** 0.35 M Lithium Sulfate, **87.5 µl** 31.5 %v/v PEG 4000, **315.0 µl** 8.0 %v/v Ethanol, **40.0 µl** Water, **32.5 µl**	[C5] 0.1 M Tris pH 7.5, **25.0 µl** 0.35 M Lithium Sulfate, **87.5 µl** 34.0 %v/v PEG 4000, **340.0 µl** 8.0 %v/v Ethanol, **40.0 µl** Water, **7.5 µl**

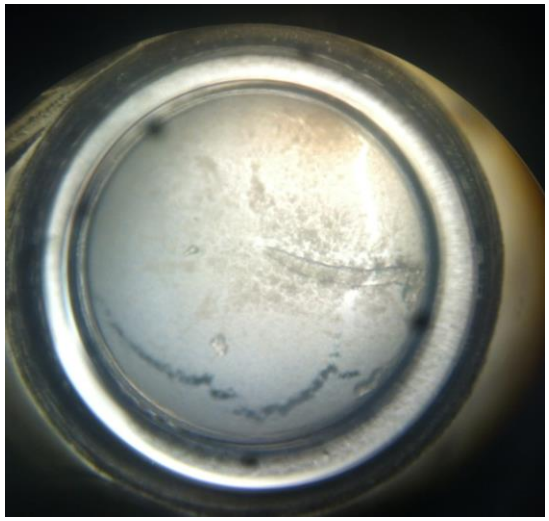

A4, II

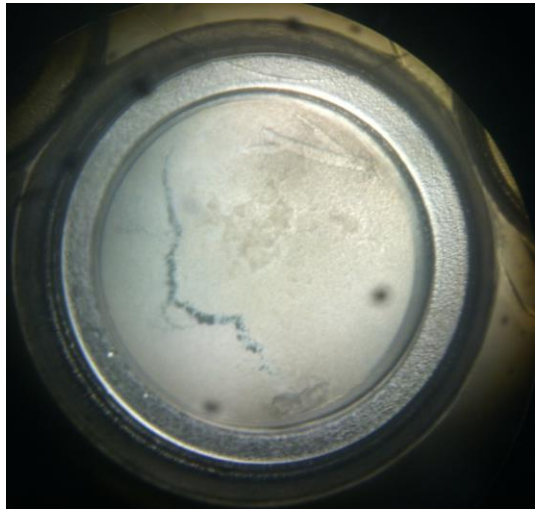

B5, II

C1, III

Figure 9

Non-volatile additive: Strontium Chloride

I: 0.075 M
II: 0.075 M
III: 0.125 M

	1	2	3	4	5
A	[A1] 0.1 M Tris pH 7.5, **25.0 µl** 0.3 M Lithium Sulfate, **75.0 µl** 22.0 %v/v PEG 4000, **220.0 µl** 8.0 %v/v Ethanol, **40.0 µl** Water, **140.0 µl**	[A2] 0.1 M Tris pH 7.5, **25.0 µl** 0.3 M Lithium Sulfate, **75.0 µl** 25.0 %v/v PEG 4000, **250.0 µl** 8.0 %v/v Ethanol, **40.0 µl** Water, **110.0 µl**	[A3] 0.1 M Tris pH 7.5, **25.0 µl** 0.3 M Lithium Sulfate, **75.0 µl** 28.0 %v/v PEG 4000, **280.0 µl** 8.0 %v/v Ethanol, **40.0 µl** Water, **80.0 µl**	[A4] 0.1 M Tris pH 7.5, **25.0 µl** 0.3 M Lithium Sulfate, **75.0 µl** 31.5 %v/v PEG 4000, **315.0 µl** 8.0 %v/v Ethanol, **40.0 µl** Water, **45.0 µl**	[A5] 0.1 M Tris pH 7.5, **25.0 µl** 0.3 M Lithium Sulfate, **75.0 µl** 34.0 %v/v PEG 4000, **340.0 µl** 8.0 %v/v Ethanol, **40.0 µl** Water, **20.0 µl**
B	[B1] 0.1 M Tris pH 7.5, **25.0 µl** 0.35 M Lithium Sulfate, **87.5 µl** 22.0 %v/v PEG 4000, **220.0 µl** 8.0 %v/v Ethanol, **40.0 µl** Water, **127.5 µl**	[B2] 0.1 M Tris pH 7.5, **25.0 µl** 0.35 M Lithium Sulfate, **87.5 µl** 2 .0 %v/v PEG 4000, **250.0 µl** 8.0 %v/v Ethanol, **40.0 µl** Water, **97.5 µl**	[B3] 0.1 M Tris pH 7.5, **25.0 µl** 0.35 M Lithium Sulfate, **87.5 µl** 28.0 %v/v PEG 4000, **280.0 µl** 8.0 %v/v Ethanol, **40.0 µl** Water, **67.5 µl**	[B4] 0.1 M Tris pH 7.5, **25.0 µl** 0.35 M Lithium Sulfate, **87.5 µl** 31.5 %v/v PEG 4000, **315.0 µl** 8.0 %v/v Ethanol, **40.0 µl** Water, **32.5 µl**	[B5] 0.1 M Tris pH 7.5, **25.0 µl** 0.35 M Lithium Sulfate, **87.5 µl** 34.0 %v/v PEG 4000, **340.0 µl** 8.0 %v/v Ethanol, **40.0 µl** Water,
C	[C1] 0.1 M Tris pH 7.5, **25.0 µl** 0.37 M Lithium Sulfate, **92.5 µl** 22.0 %v/v PEG 4000, **220.0 µl** 8.0 %v/v Ethanol, **40.0 µl** Water, **122.5 µl**	[C2] 0.1 M Tris pH 7.5, **25.0 µl** 0.37 M Lithium Sulfate, **92.5 µl** 25.0 %v/v PEG 4000, **250.0 µl** 8.0 %v/v Ethanol, **40.0 µl** Water, **92.5 µl**	[C3] 0.1 M Tris pH 7.5, **25.0 µl** 0.37 M Lithium Sulfate, **92.5 µl** 28.0 %v/v PEG 4000, **280.0 µl** 8.0 %v/v Ethanol, **40.0 µl** Water, **62.5 µl**	[C4] 0.1 M Tris pH 7.5, **25.0 µl** 0.37 M Lithium Sulfate, **92.5 µl** 31.5 %v/v PEG 4000, **315.0 µl** 8.0 %v/v Ethanol, **40.0 µl** Water, **27.5 µl**	[C5] 0.1 M Tris pH 7.5, **25.0 µl** 0.37 M Lithium Sulfate, **92.5 µl** 34.0 %v/v PEG 4000, **340.0 µl** 8.0 %v/v Ethanol, **40.0 µl** Water, **2.5 µl**

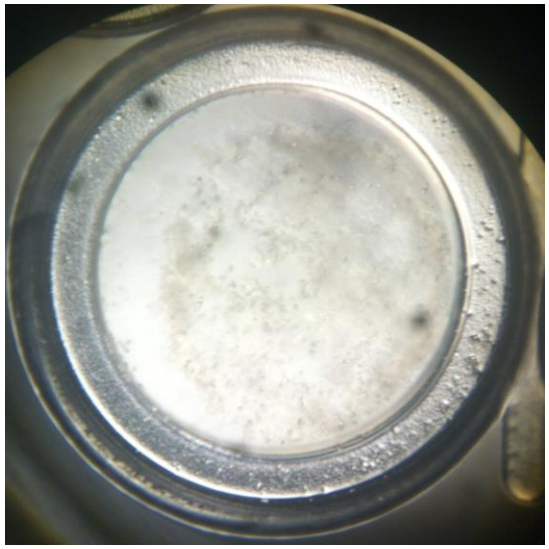

A1, III

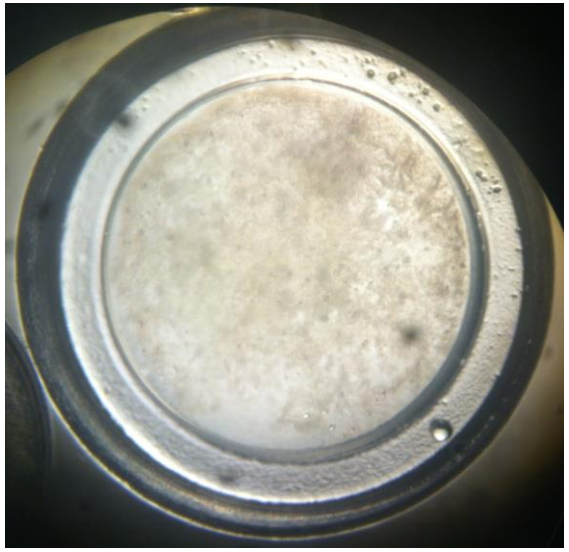

A3, II

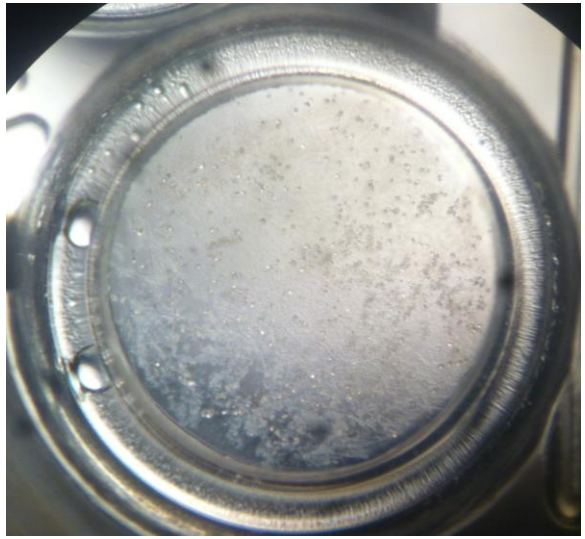

C1, III

References

1. Yoneyama H., and Katsumata R. Antibiotic Resistance in Bacteria and Its Future for Novel Antibiotic Development. *Biosci. Biotechnol. Biochem*. 2006;70(5):1060-1075.

2. Colson A. The Antibiotic Pipeline. *Extending the Cure*. 2008;6(1):1-4.

3. Facts About Antibiotic Resistance. Infectious Diseases Society of America Web site. http://www.idsociety.org/IDSA/Site_Map/Topics_of_Interest/Antimicrobial_Resistance/Public_Policy/Facts_about_Antibiotic_Resistance.aspx. Accessed March 3, 2013.

4. Invasive Candidiasis Statistics. Centers for Disease Control Web site. http://www.cdc.gov/fungal/diseases/candidiasis/invasive/statistics.html. Accessed March 3, 2013.

5. Pfaller M.A., and Diekema D.J. Rare and Emerging Opportunistic Fungal Pathogens: Concern for Resistance byond *Candida albicans* and *Aspergillus fumigatus*. *J Clin Microbiol*. 2004;42(10):4419-4431.

6. Butts A., and Krysan D.J. Antifungal Drug Discovery: Something Old and Something New. *PLoS Pathog.* 2012;8(9): e1002870.

7. Cody V., Pace J., Piraino J., Queener S.F. Crystallographic Analysis Reveals a Novel Second Binding Site for Trimethoprim in Active Site Double Mutants of Human Dihydrofolate Reductase. *J Sruct Biol*. 2012;176(1):52-59.

8. Clardy J., Fischbach M., Currie C. The natural history of antibiotics. *Curr Biol*. 2009;19(11):R437-R441.